RESEARCH PAPER

Formulation and Evaluation of Nanoemulsion: Exploring the Synergistic Antibacterial Potential of Vaccinium Macrocarpon, Cinnamomum Verum and Tribulus Terrestris for the Management of Urinary Tract Infection.

Mukesh Kumar[1]*, Divya Pathak[1]

[1]*Department of Pharmacy, IIMT College of Medical Sciences, IIMT University, Ganga Nagar, Meerut, 250001*

Received: 2nd Jun, 2025; Revised: 27th Aug, 2025; Accepted: 29th Sep, 2025; Available Online: 30th Nov, 2025

ABSTRACT

Background: Urinary tract infections (UTIs), including bladder infections (cystitis), are some of the most prevalent bacterial illness. They often require prolonged antibiotic therapy, which may contribute to antibiotic resistance and adverse side effects. To address this challenge, herbal-based nanoemulsions offer a promising alternative, leveraging natural antibacterial agents and enhancing drug delivery through nanoscale formulations.

Objective: This study aims to formulate and characterize a stable nanoemulsion incorporating Vaccinium macrocarpon, Cinnamomum verum, and Tribulus terrestris, targeting synergistic antibacterial action and enhanced drug release for effective UTI management.

Method: Nanoemulsions were formulated using the aqueous titration method, with cis-9-octadecenoic acid (oleic acid) serving as the oil component, Tween 20 as the emulsifying agent, polyethylene glycol 400 is acting as the co-emulsifier. Different Smix ratios, varying from 1:1 to 4:1, were employed to create pseudo-ternary phase diagrams. To optimize, a 12-formulation Box-Behnken factorial design was adopted. Globule size, zeta potential, pH, Consistency (viscosity), refractivity, PDI, and IVRT testwere all evaluated for the formulations.

Results: The improved nanoemulsion exhibited a transparent and monophasic nature, with A globule's size of 95.7 nanometre and a PDI of 0.95, indicating uniform distribution. The pH and refractive index were 6.5 ± 0.22 and 1.33 ± 0.05, respectively. Investigations of in vitro release test (IVRT) demonstrated controlled and sustained drug release, with the C2 formulation showing the highest cumulative release (96.3%) after 60 minutes.

Conclusion: The formulated nanoemulsion demonstrated promising physicochemical stability and enhanced in-vitro drug release, indicating that it may be a novelherbal-based beneficial strategy for effective UTI treatment.

Keywords: *Herbal nanoemulsion, Urinary Tract Infection, Synergistic antibacterial activity, Vaccinium macrocarpon, Cinnamomum verum, Tribulus terrestris, In-vitro drug release.*

How to cite this article: Kumar M; Pathak D; Formulation and Evaluation of Nanoemulsion: Exploring the Synergistic Antibacterial Potential of Vaccinium Macrocarpon, Cinnamomum Verum and Tribulus Terrestris for the Management Of Urinary Tract Infection...Int J Drug Deliv Technol. 2025;15(4): 1612-1631, DOI: 10.25258/ijddt.15.4.14

Source of support: Nil.

Conflict of interest: None

INTRODUCTION

Millions of people around the world suffer from urinary tract infections (UTIs), particularly bladder infections, making them one of the most common infectious diseases.They are responsible for a significant percentage of bacterial infections that are seen in both hospital and community settings. Both men and women may have UTIs, but women are far more vulnerable because of anatomical and physiological variables[1]. These infections can range from uncomplicated lower UTIs, such as cystitis, to more severe upper UTIs like pyelonephritis. The most frequent pathogens are *Klebsiella pneumoniae, Escherichia coli*, *Proteus mirabilis*,*coagulase-negative staphylococcus* (*Staphylococcus saprophyticus*.) Among these, *Escherichia coli*remains predominant pathogen, implicated in over 80% of uncomplicated UTIs[2]. The conventional management of UTIs largely relies on the use of antibiotics, including trimethoprim-sulfamethoxazole, nitrofurantoin, fluoroquinolones, and beta-lactam antibiotics. fortunately the effectiveness of these therapies has been seriously harmed by the increasing appearance of strains that are resistant to antibiotics[3]. Multiresistance, extended-broad-spectrum beta-lactamases (ESBLs) production, and carbapenem resistance have become widespread, posing significant clinical and public health challenges. This crisis has prompted researchers to explore novel strategies for combating UTIs beyond traditional antibiotic therapies[4]. One promising approach is the utilization of medicinal plants and herbal constituents known for their antimicrobial properties. Numerous biological functions are shown by phytochemicals, such as antimicrobial and anti-inflammatory, antioxidant and immunomodulatory effect[5].

**Author for Correspondence:* mukeshkmr681@gmail.com

Table 1: Organoleptic properties of VM, CV and TTL				
Sr. No.	Parameter	Inferences		
		VM	CV	TTL
1	Nature	Crystalline powder	Amorphous powder	Amorphous powder
2	Odor	odorless	odorless	Odorless
3	Colour	Read	Greenish	Yellow to light brown
4	Taste	Bitter	Sweet	Bitter

Their structural diversity and multifaceted mechanisms of action provide a valuable alternative to synthetic drugs, particularly in the face of antimicrobial resistance. Vaccinium macrocarpon (cranberry), Cinnamomum verum (cinnamon), and Tribulus terrestris are among the medicinal plants that have attracted significant interest for their potential role in managing urinary tract infections[6].

Cranberry (Vaccinium macrocarpon) is well-documented for its properties that prevent sticking that inhibit the extraintestinal pathogenicEscherichia coli's adherence to urothelium[7]. This action is attributed to the presence of proanthocyanidins (PACs), particularly A-type PACs, which prevent bacterial colonization and subsequent infection[8].

Cranberry exhibits mild antimicrobial and antioxidant activities, making it a valuable prophylactic agent in UTI prevention[9].*Cinnamomum verum*, commonly known as true cinnamon, contains bioactive constituents such as cinnamaldehyde, eugenol, and cinnamic acid, which have demonstrated strong microbial inhibition against extensive range of bacterial and fungal pathogens[10]. Cinnamaldehyde, in particular, disrupts microbial cell membranes, interferes with enzyme function, and impairs bacterial quorum sensing. Its broad-spectrum antibacterial effect, coupled with its ability to synergize with other agents, underscores its relevance in phytotherapeutic formulations[11]. *Tribulus terrestris*, traditionally used in Ayurvedic and Unani medicine, is recognized for its diuretic, antimicrobial, and anti-inflammatory properties [12]. The plant is rich in saponins, flavonoids, and alkaloids, which underlie its curative benefits. Scientific investigations reveal that the extracts of *Tribulus terrestris* exhibit antimicrobial antibacterial action towards microorganisms that are both Gram negative (-ve) and Gram positive (+ve), making it a

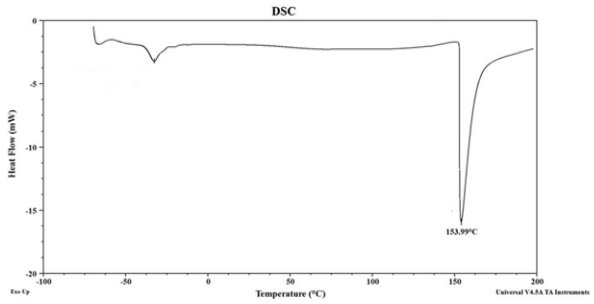

Figure 1: DSC of Vaccinium Macrocapon.

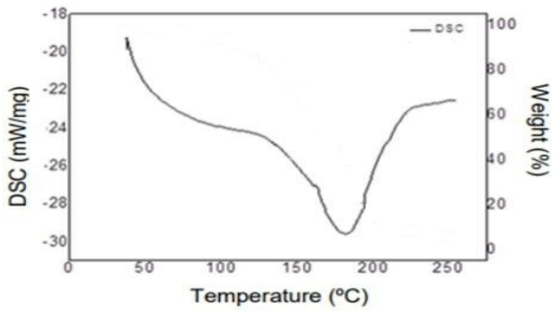

Figure 2: DSC of Cinnamomum Verum (CV)

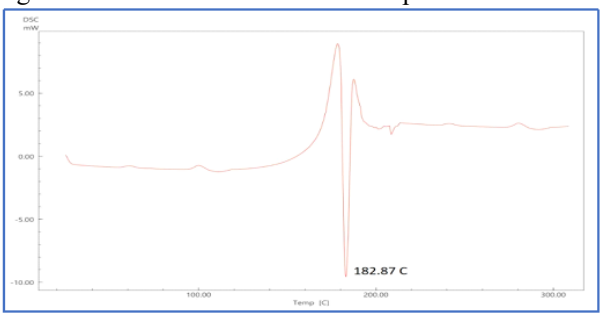

Figure 3: DSC of Tribulus Terrestris L

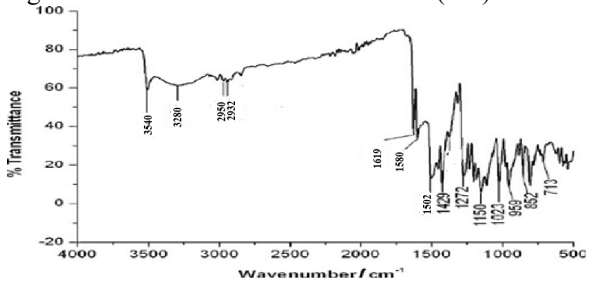

Figure 4: FTIR spectra of Vaccinium macrocapon (VM).

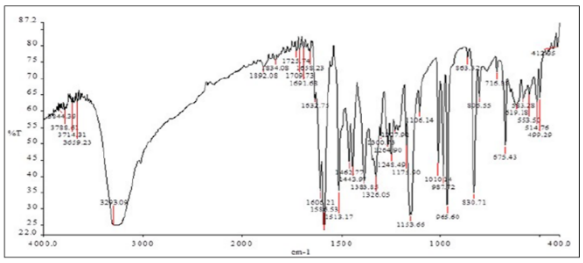

Figure 5: FTIR Spectra of Cinnamomum Verum (CV)

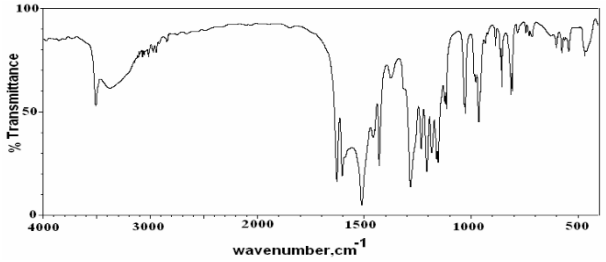

Figure 6: FTIR spectra of Tribulus Terrestris L (TTL)

suitable adjunct in herbal formulations for UTI treatment[13]. Despite their promising antimicrobial potential, herbal extracts often face limitations in terms of bioavailability, solubility, stability, and targeted delivery[14]. These challenges can be addressed by incorporating them into nanocarrier systems, particularly nanoemulsions. Emulsions with fine dispersion fall under the category of colloidal dispersions due to their particle size and distribution characteristics,comprising nanoscale droplets of oil and water stabilized by surface-active agent and co-surfactants [15]. They offer numerous advantages, including enhanced solubility and permeability of hydrophobic compounds, improved pharmacokinetics, controlled drug release, and increased stability against environmental degradation [16]. Nanoemulsions also facilitate better penetration through biological membranes, making them suitable for both oral and topical applications[17]. Furthermore, their small droplet size increases surface area, allowing for higher interaction with microbial cells and improved antibacterial efficacy [18]. These features make nanoemulsions an ideal platform for delivering phytoconstituents in the treatment of infections like UTIs. The synergistic effect of combining multiple plant extracts within a nanoemulsion system further enhances the antimicrobial efficacy, often surpassing the activity of individual components. Synergism results from complementary mechanisms of action, enhanced bioavailability, and reduced likelihood of resistance development. This concept is particularly valuable in developing alternative therapies for MDR infections.This research, therefore, seeks to develop and analyze a nanoemulsion-based delivery system encapsulating ethanolic extracts of *Vaccinium macrocarpon*, *Cinnamomum verum*, and *Tribulus terrestris*. The primary aim is to examine the effect of antibacterial potential of the combined extracts against common UTI pathogens. The study encompasses formulation optimization, physicochemical characterization, and in vitro antibacterial evaluation using agar well diffusion, MIC determination, and checkerboard synergy assays. Through this research, we seek to contribute to the development of an innovative, plant-based nanoformulation that offers enhanced therapeutic efficacy, improved delivery, and a viable alternative to conventional antibiotics for the treatment of UTIs [19].

MATERIALS AND METHODS

Materials

Vaccinium macrocarpon (VM) and *Tribulus terrestris L.* (TTL) were obtained from The Avan Company Pvt. Ltd., while *Cinnamomum verum* (CV) was procured from IIMT College of Medical Sciences. Acetonitrile (UPLC grade) was purchased from Sisco Research Laboratory Pvt. Ltd., and methanol (UPLC grade) was acquired from Merck, Mumbai, India. Additional methanol (laboratory grade), NaCl, Na_2HPO_4, Potassium dihydrogen phosphate, Polyoxyethylene Sorbitan Monolaurate (Tween 20), oleic acid, PEG 200, and iso-propanol were all procured from SDFCL, Mumbai, India. Ethyl alcohol (99.9%) was sourced from Sigma-Aldrich Chemicals Private Ltd., while Ultra-pure water suitable for UPLC analysis was procured from Loba Chemical Pvt. Ltd., Mumbai, India. Diethyl ether was obtained from Merck, Mumbai. All reagents and chemicals utilized in this study were either analytical grade or UPLC grade and were used directly without additional purification. Rhodamine B (Tetraethylrhodamine) dye was acquired from MilliporeSigma, Delhi, India, whileβ-Aminoisobutyl alcoholwas acquired from Advancion, Germany.

Methodology

Physical characterization and Identification of Vaccinium macrocapon (VM), Cinnamomum verum (CV) and Tribulus Terrestris L (TTL)

The physiochemical properties of the collected samples of Tribulus terrestris L (TTL), Cinnamomum verum (CV), and Vaccinium macrocapon (VM) were evaluated, including their hue, scent, and ability to dissolve in water and other solvents. Experiments were conducted to determine the melting point and analyse the samples using FTIR, DSC, and UV spectroscopy. The obtained findings were then compared to those reported in existing literature [19].

Examination of organoleptic properties

The composition, colour, and odour of Vaccinium macrocarpon (VM), Cinnamomum verum (CV), and Tribulus Terrestris L (TTL) were analysed and described [20] .

Examination of Melting Point

The capillary technique was used to determine the melting point of the materialand specialised melting point equipment. The capillary was filled with a sufficient amount of pharmaceutical powder, resulting in a height of 4-6 mm within the column [21]. The melting point apparatus was equipped with a capillary tube housed inside a calibrated thermometer. An individual observed the specific temperature at which a medication underwent the process of melting [22].

Examination of DSC (Differential Scanning Calorimeter)

A DSC system employing the heat-flux technique, which is made in Massachusetts, USA, was the differential thermal analyzer (DTA) utilized in this investigation. The DSC pan was used to transfer the individual samples of VM, CV, and TTL, each weighing about 2 mg, and to secure them using the DSC loading puncher. The samples were scanned between 30 and 35 °C at an average temperature rise of 10 °C/min while being exposed to nitrogen (N_2) atmosphere andDelivered at a constant rate of 60 mL per minute. A vacant pan was used as a point of reference [23].

FTIR spectroscopy served as the analytical method for assessment.

The VM, CV, and TTL samples were analysed utilising the Potassium Bromide (KBr) pellet procedure using an FTIR spectrophotometer (IR Prestige-21 Shimadzu Crop, Japan) to record their spectra. The pellet was formed by carefully mixing KBr with VM, CV, and TTL (1mg) in a (1:1) ratio,

using a hydraulic press. To enable comparison with the standard reference for analysis, the characteristic and observed spectra of The spectrum of wavelengths in which the particles were determined was 4000–400 (cm^{-1}) [24].

Validation parameter

The method was evaluated based on key validation parameters, including linearity, specificity, accuracy, precision, robustness, Together with the detection threshold (LOD) and quantification threshold (LOQ). The assessment adhered to the recommendations specified in ICH Q2 (R1).The method is evaluated to ensure its acceptance and reliability for routine use in determining the percentage content of active components in a pharmaceutical formulation after the appropriate separation conditions are met [25].

Linearity and range

Linearity of VM, CV and TTL was investigated with a concentration range of 1-6 µg/ml using stock solution with serial dilution and graph plotted between concentrations of drug against peak area. Further, linearity was determined by least-squares regression method. Above mentioned procedure was repeated in triplicate for the detection of inter-day variation throughout the course of three days.

Accuracy

Accuracy reflects how closely the calculated values align with the established reference values, demonstrating the method's reliability in producing precise results.It was defined as the relative error between nominal solution concentrations. Recovery experiments using the conventional addition approach were used to assess accuracy. Pre-analyzed samples were spiked with additional amounts of standard VM, CV, and TTL at concentrations corresponding to 50%, 100%, and 150% levels. To ensure consistency and reliability, the experiment was performed in triplicate, and the resulting mixtures were analyzed using the established method [26]. Accuracy in terms of % recovery was determined by using the formula given below.

$$\%\ \text{Recovery} = \frac{\text{Experimentally determined concentration}}{\text{Theoretical concentration}} \times 100$$

Detection limit (LOD) and quantification limit

Determination of LOD and LOQ was carried out using the signal-to-noise ratio strategy, as follows:

$$\text{Limit of Detection} = \frac{\text{Std. Deviation} \times 3.3}{\text{Slope}}$$

$$\text{Limit of Quantification} = \frac{\text{Std. Deviation} \times 10}{\text{Slope}}$$

Development of Nanoemulsion Formulation

Screening of excipients (Co-surfactant, surfactant, and oil)

When developing a mixture for gentamicin sulfate nanoemulsion, much attention will be paid to describing the drug's and the excipients' physical, chemical, and biological characteristics [27]. The drug loading capacity in nanoemulsion plays a crucial role in screening the oil phase. Higher drug sample solubility in the oil phase is often favored. In order to aid in the creation of the nanoemulsion formulation, the medication must also combine uniformly with surfactants and co-surfactants.

In an Eppendorf tube, 1.0 ml of the selected oil phase was mixed with 54 mg of the medication for oil screening.The system was allowed to reach drug equilibration over a span of 4 weeks at a constant temperature. This meticulous process aims to identify the most suitable oil phase based on the drug's solubility and compatibility with surfactants and co-surfactants for the subsequent nanoemulsion formulation.

To formulate the nanoemulsion, the surfactant plays a pivotal role in its preparation. Non-ionic surfactants were specifically chosen for the creation of the nanoemulsion due to their exceptional capabilities in development and ease of miscibility with the selected components. The selection of non-ionic surfactants was also motivated by their lower toxicity and enhanced safety compared to cationic and anionic surfactants [28].

Tween 20 and Tween 80 were specifically chosen as they exhibit maximum solubilization capacity for the drug and demonstrate high miscibility with the oil phase. These surfactants, being non-ionic in nature, are well-suited for the intended nanoemulsion formulation, contributing to its stability and efficacy. In the process of creating nanoemulsion formulations, the co-surfactant plays a crucial role due to its high miscibility with both oil and surfactant. The reason for this is because both of these chemicals are present. This is accomplished by lowering the interfacial tension between the oil phase and the surfactant blend, thereby facilitating the formation of a stable nanoemulsion. The co-surfactant used for this particular experiment was chosen based on its potential to significantly improve the drug's solubilization and demonstrate its mutual miscibility.

Depending on the extent to which they dissolved the drug, lipidic excipients were put through rigorous testing in order to create the nanoemulsion forVaccinium macrocarpon, Cinnamomum verum, and Tribulus terrestris. This step was performed to confirm the compatibility between the formulation objectives and the selected lipid-based excipients.

Diagram of the Pseudo Ternary Phase

Northeastern zone was recognized by generating pseudoternary phase diagrams using the spontaneous emulsification method, which depends on the aqueous titration approach. Surfactant and co-surfactant selection was guided by the impact of different nanoemulsion components observed in the phase diagrams, aiming to achieve optimal stability and efficient nanoemulsion formation. Considering various Smix ratios, a thorough examination of phase diagrams has shown the optimal concentration ranges for surfactants and cosurfactants(1:1, 2:1, 3:1, 4:1, 1:2, 1:3, 1:4) after their selection. For every Smix ratio, the oil to Smix ratio was adjusted.Utilizing highest ratio in a total of 12 distinct oil and Smix combinations, the border of the phase in the phase diagrams was precisely located(1: 8, 1: 7, 1:6, 1:5, 1:4, 1:2, 1:2.3, 1:2, 1:1.5, 1:1, and 1:0.7. By progressively mixing the aqueous

phase with the oil phase and Smix (surfactant combination) at varying weight ratios while gently stirring, a clear and pourable nanoemulsion (NE) was created.The formation of the NE was confirmed by visual inspection. Phase diagrams were created via Pro Sim software. The pseudoternary phase diagram shows the NE region at a constant mass ratio. Each axis in the NE represents the aqueous phase, oil phase, and Smix ratios separately [29].

Preparation of nanoemulsion formulation

The nanoemulsion (NE) containing the drug was formulated through the aqueous titration technique. Oleic acid, Tween 20, and PEG 400 were chosen as the oil phase, surfactant, and co-surfactant, respectively, due to their excellent emulsifying properties. It was found that VM was 0.67 µg/mL soluble in water but CV was 0.0034 µg/mL soluble.TTL exhibited a solubility range of 561–679 µg/mL. A water-based oil-in-water (O/W) nanoemulsion was developed using the self-assembling emulsification method. A vortex mixer (Nirmal International, Delhi, India) was used to dissolve specific quantities of VM, CV, and TTL before the Smix mixture was combined with the oil phase. The process involved maintaining the temperature at 40°C for five minutes, followed by continuous vortexing for fifteen minutes. To achieve a clear and uniform nanoemulsion, a specific amount of distilled water was gradually added while stirring continuously [30].

Table 2: Prominent Peaks of Vaccinium macrocapon in FTIR spectra

S. No.	Peak of drug sample (cm^{-1})	Pure drug peak (cm^{-1})	Name of the group
1	3658.40	3540	OH stretching
2	1685.23	1580	C=O stretching
3	1153.71	1150	C-O stretching
4	959.35	959	Olifenic bond

Table 3: Prominent Peaks of Cinnamomum Verum (CV) in FTIR spectra

S. No.	Peak of drug sample (cm^{-1})	Pure drug peak (cm^{-1})	Name of the group
1	3659.23	3674.23	OH stretching
2	1691.68	1695.77	C=O stretching
3	1320.05	1319.25	C-O stretching
4	830.71	825.02	Olifenic bond

Table 4: Prominent Peaks of Tribulus Terrestris L (TTL) in FTIR spectra

S. No.	Peak of drug sample (cm^{-1})	Pure drug peak (cm^{-1})	Name of the group
1	3741.57	3742.61	OH stretching
2	1656.24	1658.77	C=O stretching
3	1242.47	1245.55	C-O stretching
4	920.53	923.43	Olifenic bond

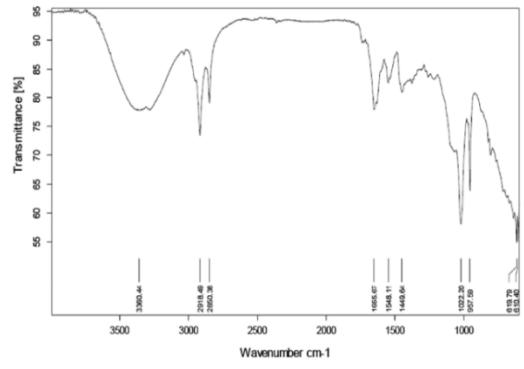

Figure 7: FTIR spectra of Vaccinium Macrocapon (VM) + Excipients

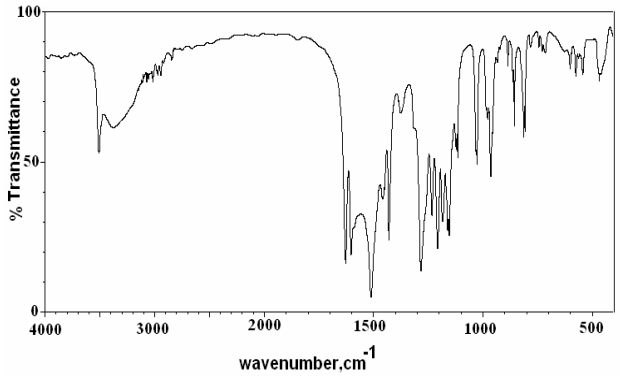

Figure 8: FTIR Spectra of Pure Cinnamomum verum (CV) + excipients

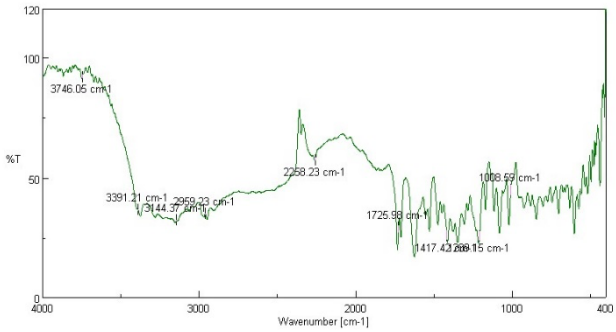

Figure 9: FTIR Spectra of Tribulus Terrestris L + Excipients

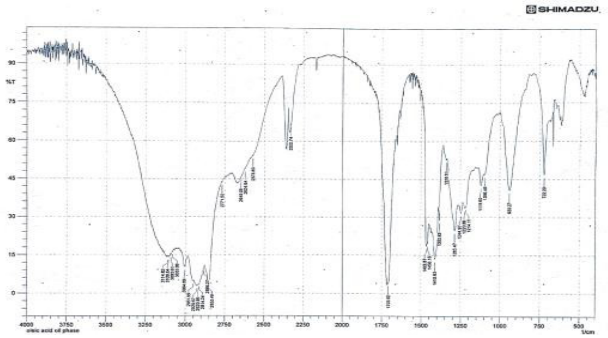

Figure 10: Oleic Acid FTIR Spectral Profile.

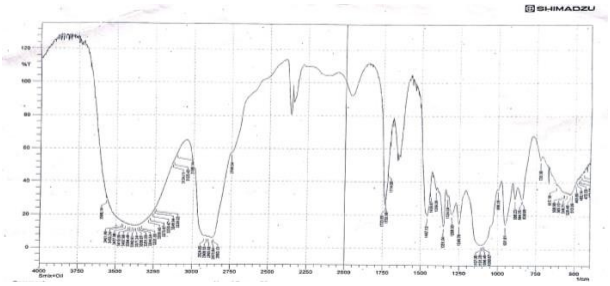

Figure 11: FTIR Spectra of Smix and Oleic Acid.

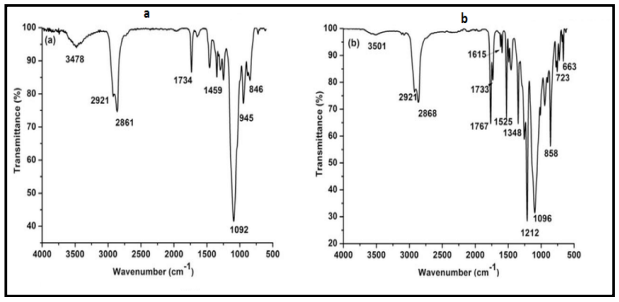

Figure 12: (a) Infrared Spectrum of Pure Tween 20 and (b) FTIR Spectra of sample Tween 20

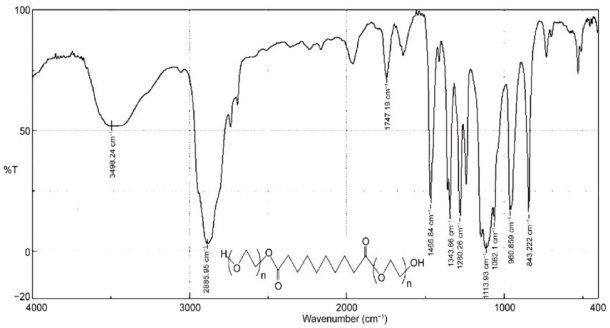

Figure 13: FTIR Spectra of PEG 400

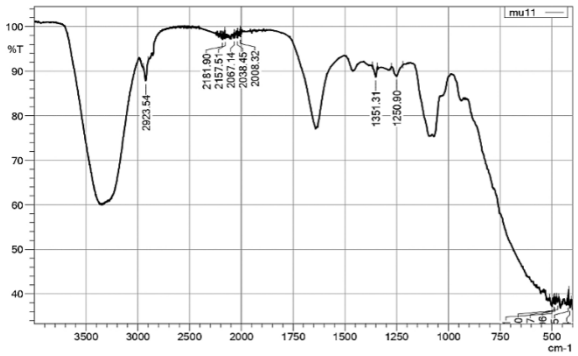

Figure 14: FTIR Spectra of Drug + Excipients

Table 5: Data for a calibration plot using linear regressionfor VM, CV, and TTL.

S. No.	Parameter	VM	CV	TTL
1	Wavelength (nm) measurement	405	288	194
2	Linear rang (µg/ml)	1-6	1-6	1-6
3	Correlation coefficient (r^2)	0.9989	0.9962	0.9979
4	LOD: Limit of Detection (µg/mL)	0.35	0.67	0.30
5	LOQ: Limit of Quantification (µg/mL)	1.03	3.1	0.89

Table 6: Recovery examination of VM, CV, and TTL

Name of sample	Measured concentration in µg/ml	Concentrations found (µg/ml) ± SD	RSD percentage	% Recovery
VM	1	0.98±0.04	0.64	98.00
	4	5.01±0.05	0.76	99.00
	6	9.07±0.15	0.85	101.01
CV	1	0.96±0.08	0.71	98.00
	4	5.13±0.19	0.69	83.23
	6	8.89±0.15	0.88	99.53
TTL	1	2.05±0.03	0.89	104.01

4	5.94±0.08	0.70	99.70
6	8.90±0.12	0.84	99.73

Table 7: Solvability profile of VM, CV and TTL across several excipients (oil surfactant and co-surfactant)

Excipient's name	Drug (Mg/ml)		
Oil	VM	CV	TTL
Oleic Acid	34.13±0.23	25.45±0.21	7.45±0.03
Almond oil	11.34±0.04	8.87±0.75	3.46±0.44
Olive oil	14.26±0.03	11.90±0.66	4.34±0.32
Castor oil	22.78±0.65	8.98±0.54	3.89±0.56
Soybean oil	17.67±0.34	9.73±0.24	3.78±0.12
Sesame oil	32.94±0.13	14.87±0.72	6.91±0.67
Surfactant			
Tween 20	32.23±0.12	17.56±0.65	10.78±0.14
Tween 80	23.43±0.56	14.54±0.16	4.67±0.57
Span 20	27.65±0.56	6.67±0.13	4.98±0.17
Span 80	22.78±0.16	5.76±0.17	3.34±0.31
Cremophore EL	29.76±0.32	7.87±0.67	5.54±0.63
Co- Surfactant			
PEG 400	35.34±0.14	18.89±0.24	45.76±0.15
PEG 200	36.34±0.39	15.84±0.90	35.42±0.17
n-Butanol	10.67±0.73	8.45±0.86	14.09±0.19
Polyethylene glycol	12.76±0.25	15.95±0.56	25.98±56

Table 8: Solubility evaluation of surfactant, co-surfactant and solvent

Surfactant	Co-Surfactant																							
	PEG 200						n-Butanol						PEG 400						Without solvent					
	O	A	C	S	S	O	O	A	C	S	S	O	O	A	C	S	S	O	O	A	C	S	S	O
Tween 20	M	M	M	S	S	M	M	M	S	S	M	M	I	M	S	S	M	M	M	M	M	M	M	M
Tween 80	I	M	S	S	M	M	M	M	S	S	M	M	S	I	S	M	M	M	S	S	S	S	S	M
Span 20	S	I	S	M	M	M	S	M	S	S	S	M	S	M	S	S	S	M	S	I	I	I	S	M
Span 80	M	M	S	S	S	M	I	M	S	S	M	M	M	M	S	M	S	M	S	I	I	I	I	M
Cremophore EL	I	I	S	I	I	S	I	M	I	I	S	M	I	S	S	S	S	S	S	S	S	S	S	S

O – Olive oil, A- Almond Oil, C- Castor oil, S – Sesame oil, S – Soybean oil, O – Oleic acid, PEG – Polyethylene Glycol, M- Miscible, I – Immiscible, S – Slightly miscible

Table 9: Trial A composition prepared using Smix (1:1) with Olive oil

Trial	Olive oil (mg)	Smix (mg)	Water (mg)	Spatial Analysis
A1	70	300	460	Clear
A2	70	300	460	Clear
A3	70	300	390	Clear
A4	70	300	320	Turbid
A5	70	300	320	Turbid

(Smix= Tween 20/ PEG 400, 1:1)

Table 10: Trial B composition prepared using Smix (1:1) with almond oil

Trial	Almond oil (mg)	Smix (mg)	Water (mg)	Spatial Analysis
B1	70	300	460	Turbid
B2	70	300	474	Turbid
B3	70	300	488	Turbid
B4	70	300	502	Turbid
B5	70	300	530	Turbid

(Smix= Tween 20/ PEG 400, 1:1)

Table 11: Trial Composition prepared using Smix (1:1) with castor oil.

Trial	Castor oil (mg)	Smix (mg)	Water (mg)	Spatial Analysis

C1	70	300	460	Turbid
C2	70	300	474	Turbid
C3	70	300	390	Turbid
C4	70	300	320	Turbid
C5	70	300	230	Turbid

(Smix= Tween 20/ PEG 400, 1:1)

Table 12: Trial Decomposition prepared using Smix (1:1) with Soybean oil.

Trial	Soybean oil (mg)	Smix (mg)	Water (mg)	Spatial Analysis
D1	70	300	460	Clear
D2	70	300	474	Turbid
D3	70	300	488	Clear
D4	70	300	502	Turbid
D5	70	300	502	Turbid

(Smix= Tween 20/ PEG 400, 1:1)

Table 13: Trial E composition prepared using Smix (1:1) with Sesame oil.

Trial	Sesame oil (mg)	Smix (mg)	Water (mg)	Spatial Analysis
E1	70	300	460	Clear
E2	70	300	474	Turbid
E3	70	300	488	Clear
E4	70	300	502	Turbid
E5	70	300	502	Turbid

(Smix= Tween 20/ PEG 400, 1:1)

Table 14: Trial F composition prepared using Smix (1:1) with oleic acid

Trial	Oleic acid (mg)	Smix (mg)	Water (mg)	Spatial Analysis
F1	70	300	460	Clear
F2	70	300	474	Turbid
F3	70	300	488	Turbid
F4	70	300	502	Turbid
F5	70	300	530	Turbid

(Smix= Tween 20/ PEG, 1:1)

Table 15: Trial G composition prepared using Smix (1:1) with oleic acid

Trial	Olive oil (mg)	Smix (mg)	Water (mg)	Spatial Analysis
G1	70	300	460	Clear
G2	70	300	474	Clear
G3	70	300	488	Turbid
G4	70	300	502	Turbid
G5	70	300	530	Turbid

(Smix= Tween 20/ PEG 200, 1:1)

Table 16: Trial H composition prepared using Smix (1:1) with oleic acid

Trial	Olive oil (mg)	Smix (mg)	Water (mg)	Spatial Analysis
H1	70	300	460	Clear
H2	70	300	474	Clear
H3	70	300	488	Clear
H4	70	300	502	Clear
H5	70	300	530	Turbid

(Smix= Tween 80/ PEG 400, 1:1)

Table 17: Trial I composition prepared using Smix (1:2) with oleic acid

Trial	Olive oil (mg)	Smix (mg)	Water (mg)	Spatial Analysis
I1	30	360	400	Clear
I2	30	360	430	Clear
I3	30	360	460	Clear
I4	30	360	580	Clear

I5	30	360	520	Clear

(Smix= Tween 20/ PEG 400, 1:2)

Table 18: Trial J composition prepared using Smix (1:3) with oleic acid

Trial	Olive oil (mg)	Smix (mg)	Water (mg)	Spatial Analysis
J1	80	360	400	Clear
J2	80	360	430	Clear
J3	80	360	460	Clear
J4	80	360	580	Clear
J5	80	360	520	Clear

(Smix= Tween 20/ PEG 400, 1:3)

Table 19: Trial K composition prepared using Smix (3:1) with oleic acid.

Trial	Olive oil (mg)	Smix (mg)	Water (mg)	Spatial Analysis
K1	80	360	400	Clear
K2	80	360	430	Clear
K3	80	360	460	Clear
K4	80	360	590	Clear
K5	80	360	550	Clear

(Smix= Tween 20/ PEG 400, 3:1)

Table 20: Trial L composition prepared using Smix (2:1) with oleic acid

Trial	Olive oil (mg)	Smix (mg)	Water (mg)	Spatial Analysis
L1	80	360	400	Clear
L2	80	360	430	Clear
L3	80	360	460	Clear
L4	80	360	590	Clear
L5	80	360	550	Clear

(Smix= Tween 20/ PEG 400, 2:1)

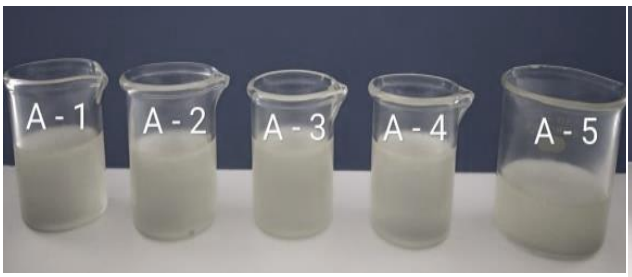

Figure 15: Pre concentrate mix consisted of Tween 20 / PEG 400 and Olive oil upon aqueous dispersion

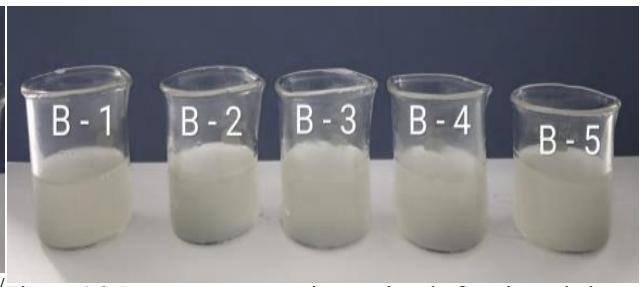

Figure 16: Pre concentrate mix consisted of Smix and almond oil upon aqueous dispersion

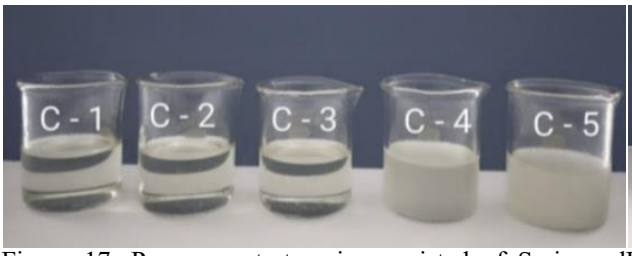

Figure 17: Pre concentrate mix consisted of Smix and castor oil upon aqueous dispersion

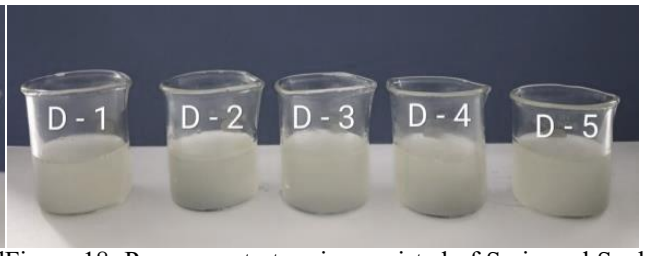

Figure 18: Pre concentrate mix consisted of Smix and Soybean oil upon aqueous dispersion

Figure 19: Pre concentrate mix consisted of Smix and sesame oil upon aqueous dispersion

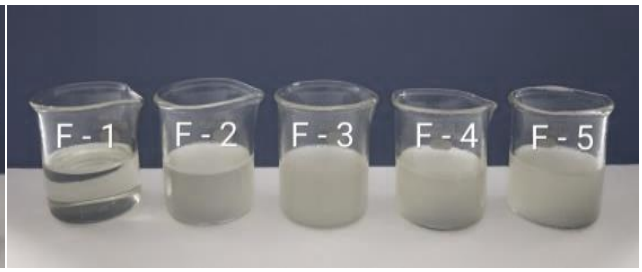

Figure 20: Pre concentrate mix consisted of Smix and oleic acid upon aqueous dispersion

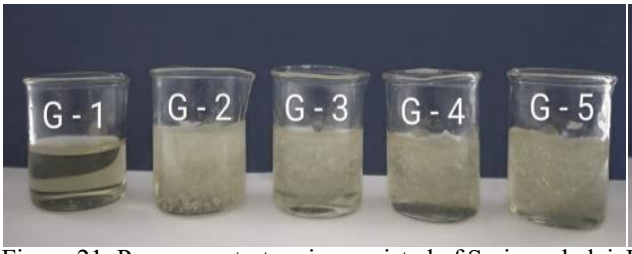

Figure 21: Pre concentrate mix consisted of Smix and oleic acid upon aqueous dispersion

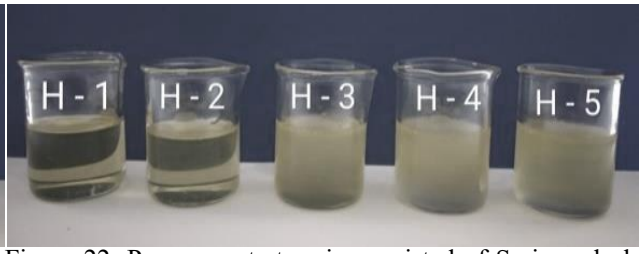

Figure 22: Pre concentrate mix consisted of Smix and oleic oil upon aqueous dispersion

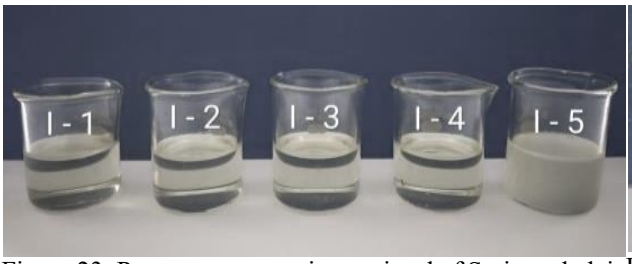

Figure 23: Pre concentrate mix consisted of Smix and oleic oil upon aqueous dilutions

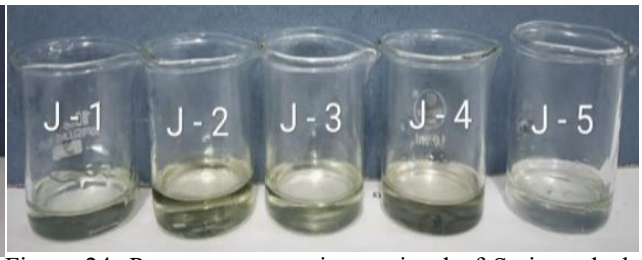

Figure 24: Preconcentrate mix consisted of Smix and oleic oil upon aqueous dispersion

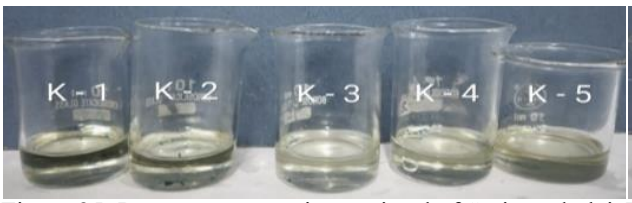

Figure 25: Preconcentrate mix consisted of Smix and oleic oil upon aqueous dispersion

Figure 26: Preconcentrate mix consisted of Smix and oleic oil upon aqueous dispersion

Table 21: Creating a Gibbs triangle or Triangular phase diagram using water, Oleic Acid (oil), 1:1 Smix ratio.

S/N	Amount of Oil (mg)	Smix (mg)	H_2O (mg)	Amount of Oil (%)	Smix (%)	H_2O (%)	Physical Inspection
1	30	110	490	0.048	0.18	0.78	Clear
2	40	80	195	0.13	0.26	0.62	Clear
3	50	70	70	0.27	0.37	0.37	Clear
4	30	90	70	0.16	0.48	0.37	Clear
5	30	160	98	0.11	0.56	0.35	Clear
6	20	100	60	0.12	0.56	0.34	Clear
7	30	130	65	0.14	0.58	0.29	Clear
8	30	150	75	0.12	0.59	0.30	Clear

Table 22: Creating a Gibbs Triangle or Triangular phase diagram at (1:2) Smix (Surfactant and co-surfactant), Oleic Acid (oil) and water.

S/N	Amount of Oil (mg)	Smix (mg)	H_2O (mg)	Amount of Oil (%)	Smix (%)	H_2O (%)	Physical Inspection

1	30	150	40	0.14	0.69	0.19	Clear
2	30	165	55	0.12	0.66	0.22	Clear
3	30	135	45	0.15	0.65	0.22	Clear
4	20	102	45	0.12	0.62	0.27	Clear
5	30	90	55	0.18	0.52	0.32	Clear
6	50	90	35	0.29	0.52	0.20	Clear
7	40	75	75	0.22	0.40	0.40	Clear
8	30	105	235	0.09	0.29	0.64	Clear

Table 23: Creating a Gibbs Triangle or Triangular phase diagram at (1:3) Smix (Surfactant and co-surfactant), Oleic Acid (oil) and water.

S/N	Amount of Oil (mg)	Smix (mg)	H_2O (mg)	Amount of Oil (%)	Smix (%)	H_2O (%)	Physical Inspection
1	30	150	108	0.11	0.53	0.38	Clear
2	20	100	65	0.11	0.55	0.36	Clear
3	30	132	45	0.15	0.64	0.22	Clear
4	30	100	45	0.18	0.58	0.26	Clear
5	30	96	55	0.17	0.54	0.31	Clear
6	50	96	35	0.28	0.54	0.20	Clear
7	40	80	75	0.21	0.42	0.39	Clear
8	30	112	235	0.08	0.30	0.63	Clear

Table 24: Creating a Gibbs triangle or Triangular phase diagram at (2:1) Smix (Surfactant and co-surfactant), Oleic acid (oil) and water

S/N	Amount of Oil (mg)	Smix (mg)	H_2O (mg)	Amount of Oil (%)	Smix (%)	H_2O (%)	Physical Inspection
1	30	165	55	0.12	0.66	0.22	Clear
2	20	99	45	0.13	0.61	0.28	Clear
3	30	135	80	0.13	0.56	0.33	Clear
4	30	99	45	0.18	0.57	0.26	Clear
5	30	105	55	0.16	0.56	0.29	Clear
6	50	105	45	0.25	0.525	0.225	Clear
7	30	90	130	0.12	0.36	0.52	Clear
8	30	114	320	0.065	0.25	0.69	Clear

Table 25: Creating a Gibbs triangle or Triangular phase diagram at (3:1) Smix (Surfactant and co-surfactant), Oleic acid (oil) and water

S/N	Amount of Oil (mg)	Smix (mg)	H_2O (mg)	Amount of Oil (%)	Smix (%)	H_2O (%)	Physical Inspection
1	20	165	45	0.09	0.72	0.20	Clear
2	30	99	35	0.19	0.61	0.22	Clear
3	20	135	70	0.09	0.6	0.33	Clear
4	20	99	40	0.13	0.63	0.26	Clear
5	30	105	45	0.17	0.59	0.25	Clear
6	50	105	35	0.27	0.56	0.19	Clear
7	30	90	120	0.125	0.375	0.5	Clear
8	20	114	310	0.05	0.26	0.70	Clear

Table 26: Creating a Gibbs triangle or Triangular phase diagram at (4:1) Smix (Surfactant, Co-surfactant), Oleic Acid (oil) and water

S/N	Amount of Oil (mg)	Smix (mg)	H_2O (mg)	Amount of Oil (%)	Smix (%)	H_2O (%)	Physical Inspection
1	30	170	50	0.12	0.68	0.2	Clear
2	20	105	45	0.12	0.62	0.27	Clear
3	30	130	70	0.14	0.57	0.31	Clear
4	30	100	40	0.18	0.59	0.24	Clear

5	20	80	35	0.15	0.59	0.26	Clear
6	50	102	30	0.28	0.57	0.17	Clear
7	20	90	110	0.091	0.41	0.5	Clear
8	20	110	315	0.045	0.25	0.71	Clear

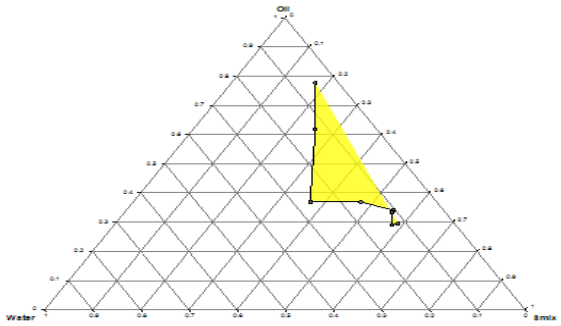

Figure 27: Triangular phase diagram constructed with 1:1 Smix, oleic acid (oil), and water.

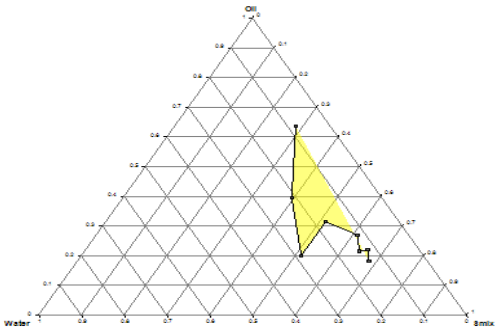

Figure 28: Triangular phase diagram constructed with 1:2 Smix, oleic acid (oil), and water.

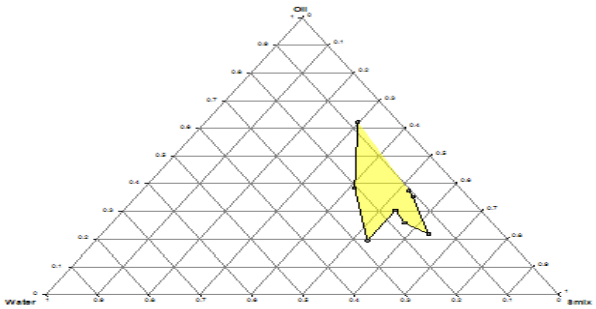

Figure 29: Triangular phase diagram constructed with 1:3 Smix, oleic acid (oil), and water.

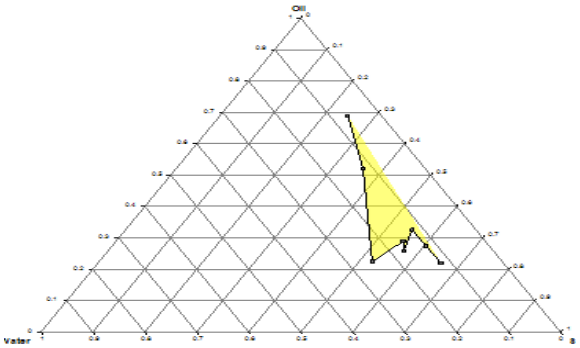

Figure 30: Triangular phase diagram constructed with 2:1 Smix, oleic acid (oil), and water.

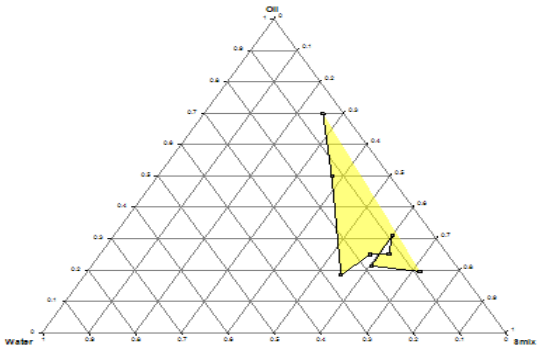

Figure 31: Triangular phase diagram constructed with 3:1 Smix, oleic acid (oil), and water.

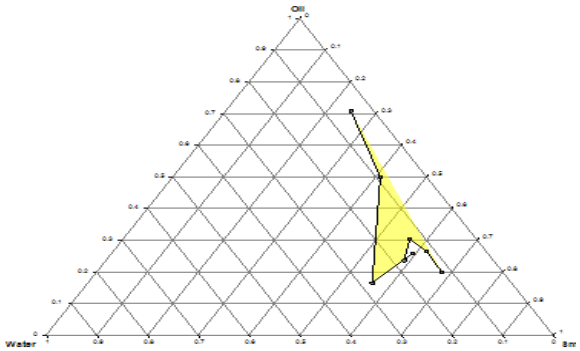

Figure 32: Triangular phase diagram constructed with 4:1 Smix, oleic acid (oil), and water.

Table 27: Ingredients of the chosen nanoemulsion formulation and their Assessment of Thermodynamic stability.

Smix ratios	Formulation code	Percent value of component (V/V)			Total Weight	Observation			Inferences
Formulation A		Oil	Smix	H_2O	110	HC	FT	Cent	Passed
Smix = ratio	A1	9	24	77	110	P	F	F	Failed

1:1	A2	8	22	85	110	P	F	P	Passed
	A3	10	25	75	110	P	F	P	Passed
	A4	12	30	68	110	P	F	F	Failed
Formulation B	B1	9	22	79	110	P	F	P	Passed
Smix = ratio	B2	12	22	76	110	F	F	F	Failed
1:2	B3	7	21	82	110	P	P	F	Passed
	B4	8	22	80	110	P	F	F	Failed
Formulation C	C1	9	19	82	110	P	F	P	Passed
Smix = ratio	C2	8	17	85	110	P	P	P	Passed
2:1	C3	10	22	78	110	P	P	F	Passed
	C4	12	32	69	110	F	P	P	Passed

Table 28: Sample Characterization Parameters for MK Size Polystyrene Latex Dispersion

Sample Name: MK size
Project Name: Data_Jul2024
Date and Time: 04 February 2025 15:22:01
Type: Size Result Source:Instrument
Cell Name: DTS0012 Temperature(°C):25
Material Name: Polystyrenelatex Dispersant Name:Water
Material RI: 1.59 Dispersant RI:1.33
Material Absorption: 0.01 Dispersant Viscosity (cP):0.887
Dispersant Dielectric Constant: 78.5

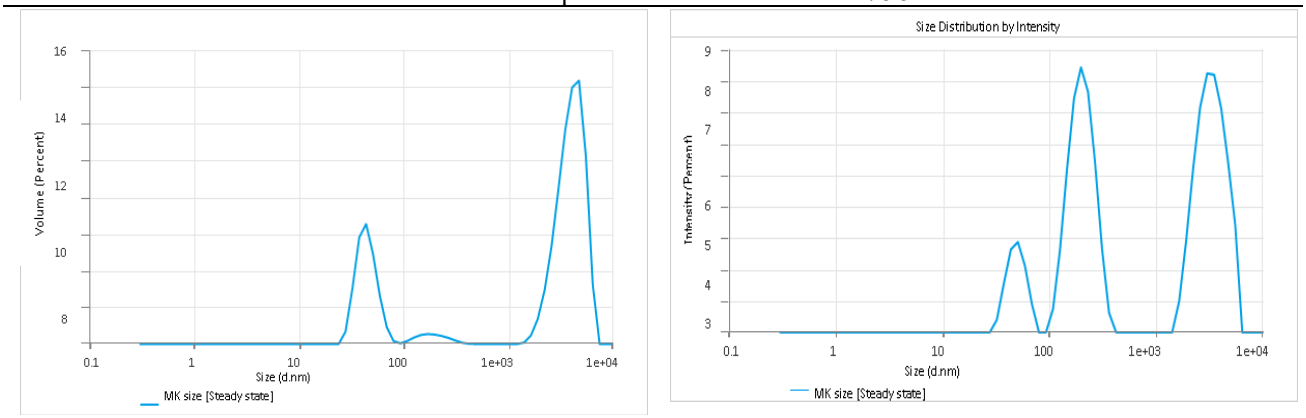

Figure 33: Globule size distribution of optimized nanoemulsion formulation

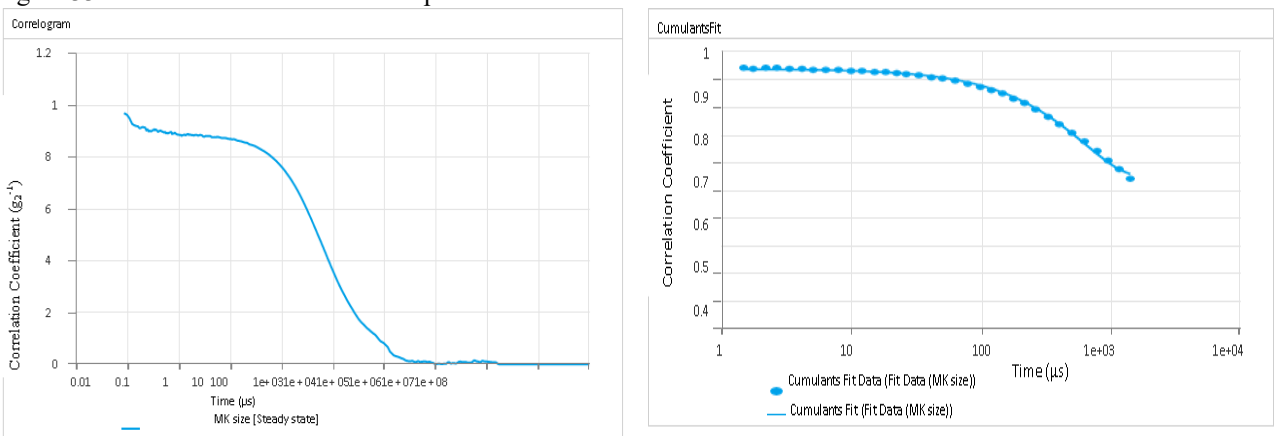

Figure 34: Poly dispersity Index analysis of optimized nanoemulsion formulation

Table 29: Statistical Analysis of Nanoemulsion Characterization Parameters

Name	Mean	Standard Deviation	RSD	Minimum	Max
Z-Average(nm)	255.4	-	-	255.4	255
PolydispersityIndex (PI)	0.9523	-	-	0.9523	0.95
Intercept	0.9355	-	-	0.9355	0.93

Fit Error	0.004121	-	-	0.004121	0.00
In Range (%)	95.77	-	-	95.77	95.7
Peak1MeanbyIntensityorderedbyarea(nm)	3350	-	-	3350	335
Peak2MeanbyIntensityorderedbyarea(nm)	204.9	-	-	204.9	204
Peak3MeanbyIntensityorderedbyarea(nm)	49.53	-	-	49.53	49.5

Table 30: Globule size, PDI, pH, RI and Viscosity analysis

Formulations	Size (nm)	PDI	pH	RI	Viscosity (mP)
A1	325.8±1.21	0.86±0.03	6.1±0.78	1.41±0.04	50.89±2.78
A2	152.3±1.45	0.94±0.06	6.6±0.76	1.36±0.07	56.77±3.09
B4	195.6±1.63	0.91±0.04	6.7±0.56	1.38±0.06	111.67±3.07
B5	134.4±1.75	0.98±0.05	6.8±0.61	1.39±0.05	121.41±4.8
C1	106.4±1.89	0.90±0.07	6.7±0.21	1.40±0.04	126.45±4.8
C2	75.7±1.34	0.75±0.06	6.5±0.22	1.33±0.05	134.3±5.02

Table 31: Zeta Potential Measurement Details for MK Zeta Polystyrene Latex Dispersion

Sample Details
Sample Name: MK Zeta
Project Name: Data_Jul2024
Date and Time: 04 February 2025 15:43:16
Type: Zeta Result Source: Instrument
Cell Name: DTS1070 Temperature(°C): 25.01
Material Name: Polystyrenelatex Dispersant Name:Water
Material RI: 1.59 Dispersant RI: 1.33
Material Absorption: 0.01 Dispersant Viscosity (cP): 0.887
Dispersant Dielectric Constant:78.5

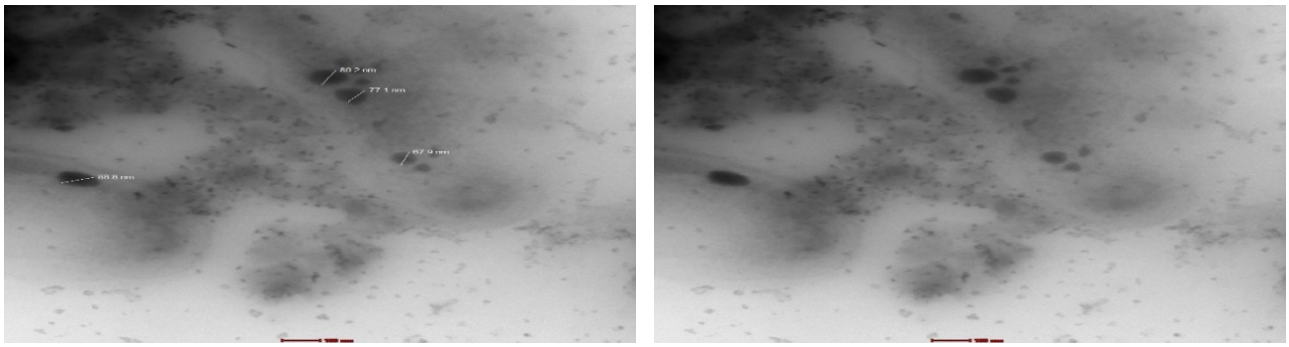

Figure 35: TEM photo graph of optimized nanoemulsion

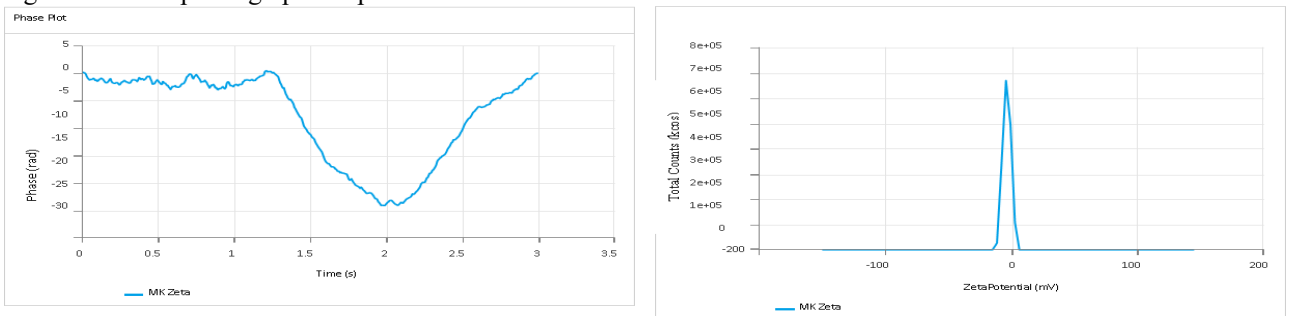

Figure 36: Zeta Potential analysis of optimized nanoemulsion

Table 32: Values of optimize nanoemulsion formulation for Zeta Potential

Name	Mean	Standard Deviation	RSD	Minimum	Maximum
ZetaPotential (mV)	-3.298	-	-	-3.298	-3.298
ZetaPeak1Mean(mV)	-3.298	-	-	-3.298	-3.298
Conductivity (mS/cm)	1.27	-	-	1.27	1.27

WallZetaPotential(mV)	-1.858	-	-	-1.858	-1.858
Zeta Deviation (mV)	3.169	-	-	3.169	3.169
Derived Mean Count Rate (kcps)	8.814E+04	-	-	8.814E+04	8.814E+04
Reference Beam Count Rate (kcps)	1162	-	-	1162	1162
Quality Factor	0.5912	-	-	0.5912	0.5912

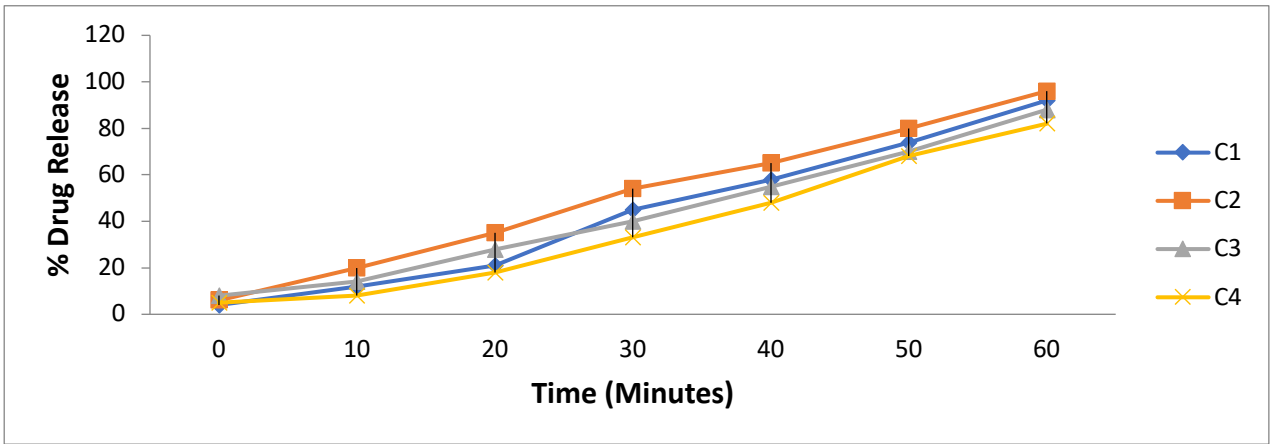

Figure 37: Investigation of In Vitro Drug Release Profiles

Evaluation of Nanoemulsion system

Thermal stability examination

To evaluate the nanoemulsion's thermodynamic stability, a modified version of Kogan and Garti's technique was used. In order to assess the formulation's resilience for long-term usage, to assess stability, the sample was put through stress conditions like centrifugation, thermal fluctuations, and freeze-thaw cycles. To guarantee the stability and dependability of the nanoemulsion, important characteristics like splitting of phases, brevity, droplets dimensions, and amount of drug were examined [31].

Evaluation of thermal cycling

The prepared nanoemulsions underwent six cycles of temperature variation, ranging from 4°C to 45°C. Each temperature setting was sustained for at least 48 hours. After completing this process, the formulations were evaluated for stability to confirm their resilience under varying thermal conditions.

Centrifugation

The NE mixtures underwent centrifugationfor 30 minutes at 3,500 revolutions per minute, and the formulations chosen for the freeze-thaw method exhibited no symptoms of Phase demarcation.

Freeze-Thaw cycle

Nanoemulsion formulations that successfully passed centrifugation tests underwent three freeze-thaw cycles, with temperatures fluctuating between -21°C and +25°C. Each cycle involved maintaining the samples at a fixed temperature for at least 48 hours to assess their stability under extreme conditions.

Evaluation of the Polydispersity Index and globule size

Two milliliters of distilled water were used to dilute around fifty microliters of the sample formulation. The globule size and polydispersity index were subsequently measured using a Zetasizer (Malvern Instruments Nano-ZS90 (Worcestershire, UK). Three distinct measuring techniques were used to estimate the average droplet size [32].

Transmission Electron Microscope (TEM)

The shape of the dispersed oil particles was examined using TEM analysis with a CM 200 microscope (Philips, based in Briarcliff Manor, New york, USA). A nanoemulsion sample, diluted at a 1:1000 ratio in water, was deposited onto a carbon-coated copper grid. To improve contrast, a 2% (w/v) phosphotungstic acid staining solution was applied. After one minute of drying, the sample was analyzed under the microscope. [33].

The Viscosity and Refractive Index

Abbe's refractometer (Precision Instruments, Germany) was used to measure the refractive index of the nanoemulsion formulation. The thickness or resistance to flow of the formulations was assessed with a Brookfield viscometer (MCR101 Rheoplus, Anton Paar India Pvt. Ltd.) to ensure precise characterization of their physical properties.

Hydrogen ion concentration (pH) and Transmittance

The pH of the formulation was determined at 25 °C using a calibrated pH meter. Using a UV-Vis spectrometer (Shimadzu UV 1601 (Japan), A volume of 1 mL from the formulation was deposited in a basins and the transmitted light was detected in triplets at 625 nm [34].

Centrifugation:

This dimension was examined in order to determine the formulation's physical stability. The nanoemulsion system was centrifuged for 10 minutes at 5000 rpm to look for any indications of creaming or phase separation. The system's appearance was examined visually after centrifugation.

In-vitro Drug Release:

In vitro drug distribution studies were conducted using a Franz diffusion cell. The filtration barrier was a pre-soaked cellophane membrane that had been conditioned in phosphate buffer for 60 minutes. It was then firmly attached to the cell. A phosphate buffer with pH 7.4 served as diffusion medium in the receiver compartment, while the nanoemulsion formulation for analysis was kept in the donor compartment. A magnetic stirrer was used continuously to keep the system at 37°C. At 10, 20, 30, 40, 50, and 60 minutes, serial sampling was carried out. To keep the receptor compartment's volume constant, new phosphate buffer was introduced. Spectrophotometric analysis was performed on the obtained samples at 262 nm [35].

RESULTS AND DISCUSSION

Physical Characterization and Identification of Vaccinium Macrocapon (VM), Cinnamomum Verum (CV) and Tribulus Terrestris L (TTL):

Organoleptic properties

Vaccinium macrocapon (VM), Cinnamomum verum (CV) and Tribulus Terrestris L (TTL) were characterized for its nature, color and odor.

Examination of melting point

By using capillary method melting point was determined for VM, CV and TTL, it was observed 184^0C, 253^0C and 44.5^0C which was near to reported value 185^0C, 254^0C and 385^0C respectively.

Examination of differential scanning calorimeter (DSC)

The DSC thermogram of VM, CV and TTL can be seen in Figure (1, 2 and 3). A sharp endothermic peak at 153.99 ºC, 195.77 ºC and 182.87 ºC was observed from DSC thermogram for CR, RS and TQ respectively, that was in agreement with the value mentioned in the literature. Therefore, it was determined that the drug sample was genuine and pure based on this investigation.

Fourier Transform Infrared Spectroscopy (FTIR)

FTIR spectra shows characteristic peaks of drug sample VM, CV and TTL mentioned in the Table 2, 3 and 4 and almost matched when compared with standard reference as shown in the Figure 4, 5 and 6

Validation Analysis

Linearity and rang

The graph of the area v/s concentration of drug sample VM, CV and TTL was found linear for the calibration plot. The coefficient of correlation R2 = 0.9989, 0.9962and 0.9979 was found which clearly indicated the linear relationship with slope and intercept values around the concentration range analyzed. The linear regression data has mentioned in Table 5.

Accuracy

To conduct the drug recovery study, standard CR, RS, and TQ were added to the previously analyzed solution at concentrations of 50%, 100%, and 150%, using the standard addition method. The recovery studies were done to estimate the CR, RS and TQ and to assess the susceptibility of the created technique. From the result it was found that the method was adequate and Table 6 showed % recovery and % RSD values. The recovery percentages for all three medications varied from 95% to 100%, and the accuracy was within acceptable ranges, with variability across all concentrations remaining below 2%. There was also no interference from any formulation components.

Quantification and Detection Limits (LOQ and LOD)

Calibration curves were further used to evaluate the responsiveness of the analytical method. LOD, the lowest concentration that could be detected by UPLC, was found to be 0.67, 0.35 and 0.30 µg/ml for VM, CM and TTL individually. LOQ, the lowest concentration that could be quantified was found to be 3, 1.03 and 0.89 µg/ml VM, CV and TTL were determined using ICH guidelines and results were shown in Table 5.

Formulation of nanoemulsion

Combination of oil, surfactant, and co-surfactant excipients

To develop an optimized nanoemulsion (NE) formulation for VM, CV, and TTL, a systematic screening of excipients, including oils, surfactants, and co-surfactants, was conducted. The primary objective was to identify components that ensure maximum drug solubility while maintaining biocompatibility and stability.Since only solubilized medications can successfully permeate the dermal layer, screening was done to find a single solvent that could dissolve all three pharmaceuticals (VM, CV, and TTL). To choose appropriate solvents for nanoemulsion (NE) formulation, the dissolution properties of each drug were evaluated in a range of oils, surfactants, and co-surfactants. Every excipient that was employed was categorized as "Generally Recognized as Safe" (GRAS).

Assessment of Drug Solubility in Oil, Smix

Oil solubility was a critical component in keeping the pharmaceuticals in a solubilized form, which was necessary to guarantee drug stability in the nanoemulsion. Table7 displays the TTL, CV, and VM solubility findings in different oils and Smix. Oleic acid was the most soluble in TTL (34.13±0.23 mg/ml), CV (25.45±0.21 mg/ml), and VM (7.45±0.03 mg/ml) among all the oils that were evaluated. The oil phase was chosen to be oleic acid because of its well-known ability to improve permeability. Because Tween 20 and PEG 400 had better solubility potential for TTL, CV, and VM, respectively, both of them were chosen to be the co-surfactant and surfactant. In Tween 20, these medications had solubility values of 32.23±0.12, 17.56±0.65, and 10.78±0.14 mg/ml, whereas in PEG 400, they were 35.34±0.14, 18.89±0.24, and 45.76±0.15 mg/mlIt takes a surfactant With an HLB score higher than 10 to generate an oil-in-water (O/W) emulsion. With an HLB value of 16.7, Tween 20 was deemed an appropriate option for this formulation.

Miscibility of excipients

Oil & Smix both are selected as per the solubility and miscibility report, shown in the table 8.

Aqueous Dispersibility of pre-concentrate mix

Constriction of Gibbs triangle (Ternary Phase diagram):

As illustrated in Figure, Pseudo-ternary phase distribution diagrams were formulated with various Smix weight ratios(Tween 20: PEG 400), including 1:1, 1:2, 1:3, 2:1, 3:1,

and 4:1. To create these graphs, Cis-Oleic Acid served as the oil phase, Polysorbate 20 (Tween 20) as the surfactant, and PEG 400 as the co-surfactant. The capacity of each Smix ratio to solubilize the oil phase and promote nanoemulsion production is the primary determinant of the nanoemulsion region's size. The nanoemulsion area was greatly decreased when Tween 20 was employed alone, emphasizing the need for a co-surfactant to minimize negative interfacial tension and generate a flexible interfacial layer. The nanoemulsion zone significantly expanded when PEG 400's was incorporated as the co-surfactant at a Smix ratio of 1:1. This result is explained by PEG 400's capacity to lower interfacial bending stress, which is essential for the stability of nanoemulsions.

Nevertheless, the nanoemulsion area shrank when the PEG 400 concentration rose in comparison to Tween 20. This decrease was probably brought on by a drop in the solubilization potential as a consequence of less micelle production. On the other hand, the nanoemulsion area increased when the PEG 400 content was lowered relative to Tween 20, suggesting better formulation stability. It was observed that there was no rise in the NE region when the Tween 20 concentration was raised in comparison to the constant PEG 400 concentration. In summary, the system's capacity to further solubilize the oil phase, lower the free energy system, and generate further emulsification resulted in the development of a sizable Isotropic region (within the nanoemulsion system) at Smix ratio 2:1 relative to the systems with varying Smix ratios. Therefore, the maximal area, as measured by the cut and weigh procedure, was shown by the Smix ratio of 2:1 and was chosen for the NE formulation.

Nanoemulsion development process

Titration using aqueous phase was employed to develop the nanoemulsion formulations. A precise ratio of surfactant to co-surfactant was carefully selected to balance nanoemulsion stability while minimizing potential skin irritation. Tween 20, A surfactant without an ionizable group, was preferred for its comparatively lower toxicity than ionic surfactants and its stability against variations in ionic strength and pH.PEG 400, used as a co-surfactant, has been reported to lower interfacial tension, contributing to the formation of a flexible and dynamic interfacial layer in the nanoemulsion. This area is full with vitality facilitates drug diffusion between phases through the surfactant film, enhancing drug partitioning and diffusion. Additionally, the presence of PEG 400 reduces the total surfactant requirement in the formulation. Based on the nanoemulsion regions identified in the phase diagram, formulations with Smix ratios of 3:1 and 4:1 were excluded because to the elevated surfactant concentrations, which could lead to inflammation of the skin. Instead, three Smix ratios 1:1 (A), 1:2 (B), and 2:1 (C) were selected for continued exploration, with the corresponding results presented in Table 27.

Thermodynamic stability

Microemulsions are stable from a thermodynamic perspective, whereas nanoemulsions exhibit kinetic stability.There are no indications of creaming, cracking, or separation of phases and are generated at certain ratios of oil, Smix, and water. To evaluate their stability, the selected formulations were subjected to a series of static tests, including as Centrifugal forces, thermal cycling, and freeze-thaw procedures.

Phase separation was observed in some formulations during physical stability tests, while others became turbid. Table 27 displays the outcomes of these examinations. Ostwald ripening, in which smaller droplets clump together via a diffusion mechanism and produce bigger droplets as a result of free surface energy, was blamed for the instability of several nanoemulsions. For more investigation, those formulations that maintained their stability without experiencing any phase separation were selected. Formulations that successfully fulfilled the requirements of the physical screening test were chosen for drug loading. VM, CV, and TTL were all dissolved in the oil phase at different amount of 3 mg/ml in order to create the drug-loaded nanoemulsion (NE). Dist. water was gradually applied dropwise to achieve a clear and transparent nanoemulsion. Physical stability testing was performed on all drug-loaded NE formulations. According to the findings, formulation C2 passed every stability test. Furthermore, C2 showed the highest overall performance, according to characterisation data from Table 27. As a result, C2 was chosen as the optimal formulation and assigned the designation DLNE for more characterisation study.

Evaluation of the produced nanoemulsion

Size of the globules and Poly dispersity Index analysis

The nanoemulsion had a uniform Poly dispersity Index (PDI) of 0.95, a dimension of the droplets 95.7 nm, and was found to be transparent and monophasic. Every NE formulation had a restricted size distribution, as seen in Table 29. This is explained by the increased surfactant content, which improves stability by forming a densely packed film along the oil–aqueous interface. The results imply that the surfactant is more important for emulsifying the oily phase than the co-surfactant. A narrower size distribution (indicated by a low PDI) signifies a better-distributed droplet size distribution, contributing to improved formulation stability and consistency.

Transmission Electron Microscopy (TEM)

The optimized nanoemulsion had no discernible aggregates and a consistent, homogenous dispersion of spherical particles, as shown in Figure17. This shows that the formulation is stable and has been emulsified effectively. The obtained outcomes further supported the nanoemulsion's homogeneity by agreeing with the globule size study carried out using the Zetasizer.

Refractive Index and Viscosity

The isotropic nature and chemical stability of the drug-loaded nanoemulsion (NE) formulations were confirmed by the almost similar mean refractive index (RI) values, as shown in Table 29. The optimized nanoemulsion's viscosity and RI were measured at 1.33 ± 0.05 mp. As anticipated for an oil-in-water (o/w) system, the drug-loaded NE formulations had a noticeably low viscosity. The inclusion of Tween 20, which has a high naturally occurring the fatty acid-polyhydric alcohol composition, is responsible for its

viscosity, and the low oil content are responsible for the low viscosity.

Transmittance and pH

A pH of 6.5 ± 0.22 was shown by the optimized nanoemulsion, suggesting formulation stability. All drug-loaded NE formulations had pH values between 6.1 and 6.7, which are appropriate for topical administration, as shown in Table 29. Interestingly, the pH of the formulations was unaffected by the addition of medications. The homogeneous dispersion of oil globules inside the continuous phase was validated by comparable transmittance values across all formulations. It was discovered that the majority of oil droplets were smaller than one-fourth of the visible light wavelength, which helped the nanoemulsion look transparent.

Zeta Potential (ZP)

The particle stability of colloids is determined by the ZP. Determining the particle's surface charge and forecasting the stability of the colloidal particle preservation depend on this crucial measurement. Indicates that the optimized nanoemulsion had a conductivity of 1.27mS/cm and a zeta potential reading of -1.858 mV. This large negative value indicates a good colloidal nature because of the nanoemulsion monotonous dispersity, outstanding stability over extended storage periods, and negative repulsion.

Centrifugation

After diluting the nanoemulsion formulation with purified water, a 15-min centrifugation was performed at 1000 rpm in a Remi centrifuge (Remi Laboratories, Mumbai, India). The formulation's resistance to physical changes under centrifugal force was next confirmed by looking for any changes in homogeneity.

Studies on In Vitro Drug Release

The samples exhibited absorbance levels that were measured spectrophotometrically at 262 nm at 5, 10, 20, 30, and 60 minutes to evaluate the administration of the medication through the cellophane membrane. In order to determine the release behavior characteristics of various formulations, in vitro % drug release tests were carried out.After 60 minutes, compositions C1, C2, C3, and C4 showed regulated drug releases of 92.1%, 96.3%, 88.2%, and 82.2%, respectively. With the greatest cumulative drug release of 96.3% among them, C2 demonstrated its superior release efficiency. It was shown that the formulation's lipid and polymer concentrations had the most effects on medication release.

CONCLUSION

The present study successfully formulated and characterized a stable herbal nanoemulsion incorporating *Vaccinium macrocarpon*, *Cinnamomum verum*, and *Tribulus terrestris*, demonstrating significant potential for urinary tract infection management. The optimized formulation exhibited desirable physicochemical properties, including small globule size, uniform distribution, appropriate pH, and excellent clarity. The in vitro drug release studies confirmed a sustained and enhanced release profile, with the C2 formulation showing the highest cumulative drug release, indicating the synergistic efficacy of the selected plant extracts. The nanoemulsion system not only improves the solubility and permeability of bioactive phytoconstituents but also offers a promising alternative to conventional antibacterial therapies, potentially reducing resistance development and side effects. These findings lay the groundwork for future in vivo evaluations and clinical translation of this herbal-based nanocarrier system for effective and patient-friendly UTI treatment.

Acknowledgements

The authors wish to convey their heartfelt appreciation to IIMT College of Medical Sciences, IIMT University, or providing the vital resources and guidance throughout this research. Special thanks to my PhD Supervisor Dr. Divya Pathak for their continuous Invaluable support and technical expertise during this work.

.

REFERENCE

1. Santos M, Mariz M, Tiago I, Martins J, Alarico S, Ferreira P. A review on urinary tract infections diagnostic methods: laboratory-based and point-of-care approaches. J Pharm Biomed Anal. 2022. doi:10.1016/j.jpba.2022.114889.
2. Ortega-Lozano AJ, Hernández-Cruz EY, Gómez-Sierra T, Pedraza-Chaverri J. Antimicrobial activity of spices popularly used in Mexico against urinary tract infections. Antibiotics. 2023;12:325. doi:10.3390/antibiotics12020325.
3. Gupta K. Acute complicated urinary tract infection (including pyelonephritis) in adults. UpToDate. 2022.
4. Elbargisy RM. Optimization of nutritional and environmental conditions for pyocyanin production by urine isolates of Pseudomonas aeruginosa. Saudi J Biol Sci. 2021. doi:10.1016/j.sjbs.2020.11.031.
5. Arsene MMJ, et al. Phytochemical analysis, antibacterial and antibiofilm activities of Aloe vera aqueous extract against selected resistant Gram-negative bacteria involved in urinary tract infections. Fermentation. 2022;8:1126. doi:10.3390/fermentation8110626.
6. Nguyen HQ, Nguyen NTQ, Hughes CM, O'Neill C. Trends and impact of antimicrobial resistance on older inpatients with urinary tract infections: a national retrospective observational study. PLoS One. 2019;14:e0223409. doi:10.1371/journal.pone.0223409.
7. Rane HS, Bernardo SM, Howell AB, Lee SA. Cranberry-derived proanthocyanidins prevent formation of Candida albicans biofilms in artificial urine through biofilm- and adherence-specific mechanisms. J Antimicrob Chemother. 2014;69:428–436. doi:10.1093/jac/dkt398.
8. Dugoua JJ, Seely D, Perri D, Mills E, Koren G. Safety and efficacy of cranberry (Vaccinium macrocarpon) during pregnancy and lactation. Can J Clin Pharmacol. 2008;15:e66–e76.
9. Iqbal A, Ibrahim M, Muhammad N. Natural

approach used for urinary tract infections. 2023.
10. De Llano DG, Moreno-Arribas MV, Bartolomé B. Cranberry polyphenols and prevention against urinary tract infections: relevant considerations. Molecules. 2020;25:3523. doi:10.3390/molecules25153523.
11. Shreya A, Manisha D, Sonali J. Phytochemical screening and antimicrobial activity of cinnamon spice against urinary tract infection and fungal pathogens. Int J Life Sci Pharma Res. 2015.
12. De Llano DG, Moreno-Arribas MV, Bartolomé B. Cranberry polyphenols and prevention against urinary tract infections: a brief review. In: Current Advances in Chemistry and Biochemistry. Vol. 4. 2021. doi:10.9734/bpi/cacb/v4/7627d.
13. Rubano A, Rabinowitz R, Ajay D. A history of four Chinese herbs used to treat acute and chronic urinary disorders. Int J Urol Hist. 2023. doi:10.53101/ijuh.3.1.092402.
14. Kwok M, et al. Guideline of guidelines: management of recurrent urinary tract infections in women. BJU Int. 2022. doi:10.1111/bju.15756.
15. Feltes G, Ballen SC, Steffens J, Paroul N, Steffens C. Differentiating true and false cinnamon: exploring multiple approaches for discrimination. Micromachines. 2023;14:1819. doi:10.3390/mi14101819.
16. Mishra MP, Rath S, Swain SS, Ghosh G, Das D, Padhy RN. In vitro antibacterial activity of crude extracts of 9 selected medicinal plants against UTI-causing MDR bacteria. J King Saud Univ Sci. 2017;29:442–449. doi:10.1016/j.jksus.2015.05.007.
17. El-Naggar ME, Abdelgawad AM, Abdel-Sattar R, Gibriel AA, Hemdan BA. Potential antimicrobial and antibiofilm efficacy of essential oil nanoemulsion loaded polycaprolactone nanofibrous dermal patches. Eur Polym J. 2023;188:111782. doi:10.1016/j.eurpolymj.2022.111782.
18. Zahoor M, et al. An ethnopharmacological evaluation of Navapind and Shahpur Virkan in District Sheikupura, Pakistan for their herbal medicines. J Ethnobiol Ethnomed. 2017;13:1–15. doi:10.1186/s13002-017-0151-1.
19. Bharanidharan R, et al. In vitro screening of East Asian plant extracts for potential use in reducing ruminal methane production. Animals. 2021;11:1020. doi:10.3390/ani11041020.
20. Khushali K, Bansi G, Samir P, Manan R. Estimation of scopoletin from a polyherbal formulation using HPLC coupled with fluorescence detector through design of experiment. Luminescence. 2023. doi:10.1002/bio.4446.
21. Kulichenko EO, et al. Obtaining a working standard sample of chalcone buteine and its quantitative determination in plant raw materials. Probl Biol Med Pharm Chem. 2024. doi:10.29296/25877313-2024-01-03.
22. Zhang H, Zhang Z, Zhao Y, Liu Y. Preparation of calcium magnesium acetate snow melting agent using raw calcium acetate-rich eggshells. Waste Biomass Valorization. 2020;11:5673–5682. doi:10.1007/s12649-019-00920-6.
23. Gill P, Moghadam TT, Ranjbar B. Differential scanning calorimetry techniques: applications in biology and nanoscience. J Biomol Tech. 2010;21:1–34.
24. Draz MS, et al. Correction to hybrid nanocluster plasmonic resonator for immunological detection of hepatitis B virus. ACS Nano. 2014;8:10165. doi:10.1021/nn505684g.
25. Thi Nghia P, Thi Hai Yen T, Thi Thu Giang V. Development of in-house specifications and study of stability of self-nanoemulsifying drug delivery system containing rosuvastatin. VNU J Sci Med Pharm Sci. 2020. doi:10.25073/2588-1132/vnumps.4254.
26. Zhang M, Cai Y, Xiao L, Wang L. Discussion on precision evaluation method of serpentine phase quantitative analysis by X-ray diffraction. Yankuang Ceshi. 2023. doi:10.15898/j.cnki.11-2131/td.202101180010.
27. Onugwu AL, et al. Nanotechnology-based drug delivery systems for the treatment of anterior segment eye diseases. J Control Release. 2023. doi:10.1016/j.jconrel.2023.01.018.
28. Rancan F, et al. Screening of surfactants for improved delivery of antimicrobials and PLGA particles in wound tissue. Pharmaceutics. 2021;13:1093. doi:10.3390/pharmaceutics13071093.
29. Ponce Ponte M, Croatto M, Longhi M, Aloisio C. Ginger oil-based microemulsion as a strategy to improve the topical therapy of imiquimod. Colloids Surf A. 2024;674:132619. doi:10.1016/j.colsurfa.2023.132619.
30. Latif MS, Nawaz A, Asmari M, Uddin J, Ullah H, Ahmad S. Formulation development and in vitro/in vivo characterization of methotrexate-loaded nanoemulsion gel formulations for enhanced topical delivery. Gels. 2023;9:3. doi:10.3390/gels9010003.
31. Uner B, et al. Loteprednol-loaded nanoformulations for corneal delivery: ex vivo permeation study, ocular safety assessment and stability studies. J Drug Deliv Sci Technol. 2023;78:104252. doi:10.1016/j.jddst.2023.104252.
32. Petrochenko PE, et al. Analytical considerations for measuring the globule size distribution of cyclosporine ophthalmic emulsions. Int J Pharm. 2018;552:239–249. doi:10.1016/j.ijpharm.2018.08.030.
33. Dlamini NG, Basson AK, Pullabhotla VSR. Synthesis and characterization of various bimetallic

nanoparticles and their application. Appl Nano. 2023;4:1. doi:10.3390/applnano4010001.

34. Montoya E, Quintero J. Sistemas de gestión de seguridad y salud en el trabajo: revisión de la normatividad vigente aplicable en Colombia. Front Neurosci. 2021. .

35. Salamanca CH, Barrera-Ocampo A, Lasso JC, Camacho N, Yarce CJ. Franz diffusion cell approach for pre-formulation characterisation of ketoprofen semi-solid dosage forms. Pharmaceutics. 2018;10:148. doi:10.3390/pharmaceutics10030148.